PAPER

Surface modification of ZnO quantum dots by organosilanes and oleic acid with enhanced luminescence for potential biological application

To cite this article: Nathalia Cristina Rissi *et al* 2017 *Mater. Res. Express* **4** 015027

Materials Research Express

PAPER

RECEIVED
8 August 2016

REVISED
5 December 2016

ACCEPTED FOR PUBLICATION
19 December 2016

PUBLISHED
30 January 2017

Surface modification of ZnO quantum dots by organosilanes and oleic acid with enhanced luminescence for potential biological application

Nathalia Cristina Rissi[1], Peter Hammer[2] and Leila Aparecida Chiavacci[1]

[1] School of Pharmaceutical Sciences, UNESP, Univ Estadual Paulista, Rodovia Araraquara-Jaú, km 1, 14801-902, Araraquara, SP, Brazil
[2] Chemical Institute, UNESP, Univ Estadual Paulista, Rodovia Araraquara-Jaú, km 1, 14800-900, Araraquara, SP, Brazil

E-mail: leila@fcfar.unesp.br

Keywords: quantum dots (QDs), ZnO, photoluminescence

Supplementary material for this article is available online

Abstract

Luminescent ZnO-QDs is a promising candidate for biological application, especially due to their low toxicity. Nevertheless, colloidal ZnO-QDs prepared by sol–gel route are unstable in water and incompatible with lipophilic systems, hindering their application in biology and medicine. To tackle the problem, this study reports three different strategies for surface modification of ZnO-QDs by: (i) hydrophilic (3-glycidyloxypropyl) trimethoxysilane (GPTMS), (ii) hydrophobic hexadecyltrimethoxysilane (HTMS) and then by (iii) oleic acid (OA) and HTMS bilayer. Capped ZnO-QDs by GPTMS and HTMS were performed by hydrolysis and condensation reactions under basic catalysis, leading to the formation of siloxane layer, involving strong interaction between the silanes with hydroxylated surface of ZnO, thereby creating a covalent bond—ZnO–O–Si. Alternatively, OA and HTMS were employed as hydrophobic agent to form a bilayer barrier surrounding the nanoparticles (NPs). Capped ZnO-QDS were analyzed by techniques including: Fourier transform infrared spectroscopy, x-ray photoelectron spectroscopy, x-ray diffraction and transmission electron microscopy, as well as the monitoring of excitonic peak of ZnO by UV–vis absorption spectroscopy. Photoluminescence measurements confirmed the importance of capping agents. Bare ZnO-QDs powder showed lowest photoluminescence intensity and displacement to yellow region when compared with ZnO-QDs capped, which present a higher photoluminescence in the green region. The above results can be related to changes of the concentration of oxygen vacancies (V_o) and also by increased presence of surface defect density. Silane capping represents the best choice for high stability and photoluminescence enhancement of ZnO-QDs.

1. Introduction

With the recent advances obtained in nanomedicine field, it is possible to observe a growing interest to develop luminescent materials for biological applications. In this regard, luminescent quantum dots (QDs) have gained considerable attention in this field [1–4].

The photoluminescence process in semiconductor QDs with a size between 2 and 10 nm [5] occurs owing to the quantum confinement of electrons and their different energy states within the band gap [6, 7]. The emission of different spectral intensities is associated to the particle size and also to defects density of the crystal structure, which relate directly to the emitted fluorescence by creating intermediate energy levels within the band gap [8]. Examples of major defects found in ZnO-QDs are oxygen vacancies (V_o) and zinc vacancies (V_{Zn}) [9]. Additionally, there are also surface defects, known as 'dangling bonds'. These defects, related to unsaturated valence of surface atoms, are known to affect the photoluminescence process by acting as interface traps with deep band-gap energy levels [10].

Therefore, one approach to reduce these defects and improve the photoluminescence efficiency of QDs is through surface passivation [11]. The surface passivation is generally performed by an inorganic or organic layers

grafted to the QDs surface. The inorganic passivation, resulting in the formation of core shell system, it is the most used methods to passivate the ZnO surface. However, also a significant number of organic passivation methods using organometallic solvents are reported, as for instance trioctylphosphine oxide (TOPO) and trioctylphosphine (TOP) capping [12, 13]. These molecules adhere to the QDs surface, reducing interparticle aggregation (spacing) and act as passivation agents [11–13]. Nevertheless, there are some disadvantages in the use of TOPO mainly related to their toxicity. To replace TOPO, oleic acid (OA), considered as less toxic and cheaper, has been widely employed as QDs modifier [14].

Another important issue of surface passivation of QDs is related to strategies to modify their behavior in different solvents. ZnO is widely used as an effective photoluminescence material, especially due to its low toxicity [15]. However, colloidal ZnO-QDs prepared by common sol–gel route are unstable in aqueous solution and tend to aggregate, thus losing their luminescent properties [16]. For this reason, many surface modification strategies have been studied in order to improve the stability of ZnO NPs [17]. Moussodia *et al* [18, 19], reported interesst-ing results for ZnO-QDs modified by organosilanes. Especially the observation of their cellular internalization in *Staphylococcus aureus* showed the potential of these QDs in acting as biological probes. According to these authors, the stability in aqueous solution, good photoluminescence performance and low cytotoxicity allows the use of these QDs in various biomedical applications. Consequently, recent research activities have been focused on organosilanes as modifier and surface passivation for the stabilisation of ZnO QDs in water. The strong affinity of organosilanes towards the hydroxylated ZnO surface leads to the formation of covalent Si–O–Zn bond, thus creating a shielding barrier of siloxane around the ZnO core [16, 20–24].

The results obtained in this work suggest that QDs capped by GPTMS—(3-glycidyloxypropyl)trimethoxysilane may have a significant contribution for the development of multifunctional probes, since their photoluminescence quantum yield and stability in aqueous solution are essential requirements for biological application. Differently, capped ZnO-QDs by HTMS—hexadecyltrimethoxysilane and oleic acid—OA/HTMS bilayer can be incorporated into theranostics systems, such as liposomes and polymeric micelles. These systems, favor the use of QDs in biological imaging, besides ability to be used as direct anticancer drugs within tumor cells, and therefore can be applied for both diagnosis and therapy.

2. Experimental

2.1. Materials

Zinc acetate dehydrate (Qhemis), lithium hydroxide (Vetec), ethanol absolute (Synth), (3-glycidyloxypropyl) trimethoxysilane—GPTMS (Sigma), hexadecyltrimethoxysilane—HTMS (Sigma), rhodamine 6G (Sigma), Milli-Q water, chloroform (Synth).

2.2. Synthesis of precursor zinc oxyacetate

The precursor was prepared using a well-established method proposed by Spanhel and Anderson [25]. The $Zn_4O(Ac)_6$ tetrameric precursor (herein after referred to as ZnAc precursor) was first prepared from an ethanolic dispersion by refluxing the solution containing 0.05 M $ZnAc_2 \cdot 2H_2O$ during 2 h at 80 °C. Then, the precursor was cooled to room temperature and then stored at −10 °C.

2.3. Synthesis of ZnO colloidal suspension

The ZnO-QDs were obtained by hydrolysis and condensation reaction (sol–gel) under basic catalysis (LiOH) at 0.5 M, which was added to precursor under magnetic stirring at 40 °C and for 40 min [25]. Then the NPs were precipitated after addition of heptane to the suspension. Finally, the obtained precipitate was centrifuged and then vacuum-dried to form a powder [26].

2.4. Capped ZnO-QDs by GPTMS and HTMS

The ZnO-QDs surface capped by organosilanes was obtained using 10 ml of ZnO colloidal suspensions each containing GPTMS or HTMS. For each molar fraction of GPTMS, the concentration of LiOH was varied according to table S1 (see supplementary data (stacks.iop.org/MRX/4/015027/mmedia)). In the case of HTMS the concentration was fixed (0.1 M) together with the LiOH amount (0.05 M). During preparation, higher concentrations of HTMS and LiOH were also tested however the formation of a very consistent white precipitate prevented the redispersion of the nanoparticles in the lipophilic solvent. Both reactions were performed separately in an ultrasound bath (15 min) at room temperature. After formation of a white precipitate the solutions were then centrifuged (4000 rpm, 15 min) and obtained NPs were vacuum-dried.

2.5. Capped ZnO-QDs by OA/HTMS bilayer

The capped ZnO-QDs by OA/HTMS bilayer was carried out using 10 ml of ZnO-QDs colloidal suspension containing 0.05 M of AO. Initially, OA coating was performed under ultrasound conditions at 60 °C and

during 5 min. Under ultrasound conditions HTMS (0.1 M) and LiOH (0.05 M) was added into the solution and after 15 min the white precipitate was washed with ethanol and then centrifuged (4000 rpm, 15 min) and vacuum-dried.

2.6. UV–vis absorption spectroscopy measurements

The absorption spectra of the ZnO-QDs colloidal suspensions in ethanol was measured using a Cary Win 4000 UV–vis spectrophotometer with a cuvette of 1 mm optical path. The spectra were recorded between 200 and 400 nm, with a wavelength increment of 1 nm and 0.2 s counting time of per point. The UV–vis spectra were corrected by the baseline obtained for the ethanol absorption spectrum.

2.7. Monitoring of excitonic peak of ZnO by UV–vis absorption spectroscopy

The stability study of capped ZnO-QDs by GPTMS in water and capped ZnO-QDs by HTMS and OA/HTMS bilayer in chloroform was determined by UV–vis measurements.

2.8. Transmission electron microscopy (TEM)

A transmission electron microscope (PHILIPS, model CM 200 SUPER TWIN) operated at 200 kV was employed to obtain the micrographs. A drop of capped ZnO-QDs was dripped on single carbon grids and kept overnight.

2.9. Photoluminescence (PL)

Photoluminescence measurements were conducted in a SPEX fluorimeter F2121 and germanium detector (North Coast Scientific Corporation). A Xenon lamp (450 W) was used as the excitation light source to record the emission spectra of the samples.

2.10. Quantum yield (QY) measurements

The QY of capped ZnO-QDs by GPTMS in water and capped ZnO-QDs by HTMS and OA/HTMS bilayer in chloroform were compared with a solution of rhodamine 6G in ethanol (QY = 95%), which is often used as reference for emission in green region.

2.11. Infrared spectroscopy (FTIR)

Absorption spectra in infrared region (4000–400 cm^{-1}) were obtained using KBr pellets with an IR Prestige-21 IR Affinity-1 FTIR-8400S spectrophotometer (Kyoto, Japan).

2.12. X-ray diffraction (XRD)

XRD were analyzed by Siemens D5000 CuK diffractometer using CuKα, $\lambda = 1.5418$ Å radiation. The diffraction intensity was measured in a 2θ range of 5°–70° with an increment of 0.1° and exposure time of 3 s per step.

2.13. X-ray photoelectron spectroscopy (XPS)

XPS was performed using the UNI-SPECS UHV Surface Analysis System equipment (LEFE—IQ/UNESP). The Mg Kα excitation line was used ($h\nu = 1253.6$ eV) and the analyzer pass energy was set to 10 eV. The inelastic background of Zn 2p, Si 2p, O1s and C1s electron core-level spectra was subtracted using Shirley's method. The composition (at.%) of the near surface region was determined with an accuracy of ±10% from the ratio of the relative peak areas corrected by Scofield's sensitivity factors of the corresponding elements. The binding energy scale of the spectra was corrected using the C1s hydrocarbon component of the fixed value of 285.0 eV. The spectra were fitted without placing constraints using multiple Voigt profiles.

3. Results and discussion

ZnO-QDs were synthesized by the sol–gel method at a hydrolysis $[OH^+]/[Zn^{2+}]$ ratio of 1,4 [25] and then the surface was modified by hydrolysis and condensation reaction under basic catalysis with (i) GPTMS and (ii) HTMS, thus leading to the formation of a capping siloxane layer. As will be shown by the FTIR and XPS results, the strong interaction between the hydroxylated silane surface and ZnO results in the formation of covalent Zn–Si–O bonds [16, 18–20, 23, 27].

Alternatively, to improve the stability of ZnO-QDs and consequently their photoluminescence intensity a coating bilayer formed by (iii) OA and HTMS was synthesized. According to Aboulaich *et al* [23], OA added to colloidal suspension, probably reacts with the NPs through hydrogen bonds, forming the first protection layer. Subsequently, siloxane groups of HTMS, hydrolyzed under basic catalysis, interact with hydroxylated groups of OA-ZnO. Finally, a condensation step of silanol group results in the formation of a second protective siloxane layer. Li *et al* [16] studied the formation a self-assembly bilayer and reported in addition to increased fluorescence intensity, in relation to unprotected QDs, an improved protection of QDs against water uptake.

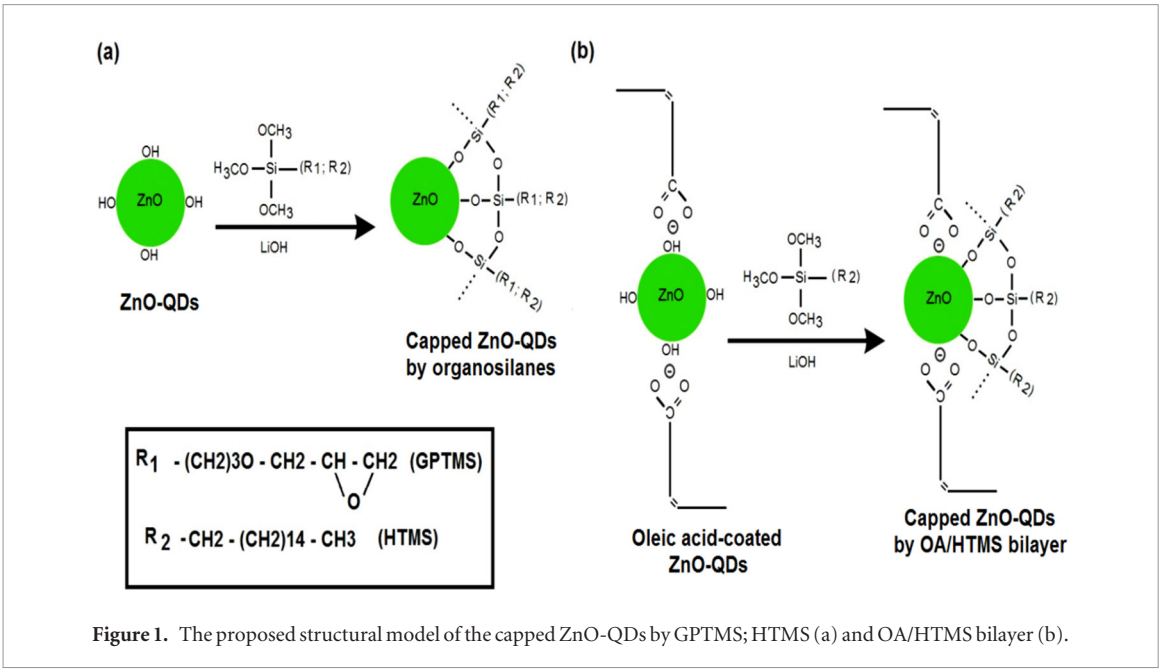

Figure 1. The proposed structural model of the capped ZnO-QDs by GPTMS; HTMS (a) and OA/HTMS bilayer (b).

The capping surface of QDs by organosilanes is already known in the literature [16, 18, 19, 23]. However, some studies present a complex synthesis that is divided in some steps. According to the Moussoudia *et al* [18, 19], and Aboulaich *et al* [23], ZnO-QDs surface modification strategy to water-dispersible begins with the synthesize of the oleate-capped ZnO-QDs dispersion in nonpolar solvent. After this step, it was necessary to exchange the oleate molecules for aminosiloxanes with amine end groups in high temperature (85 °C). Finally, the resulting hydrophilic ZnO-QDs were precipitate in nonpolar medium and isolated by centrifugation.

Thereby, our proposed method for capping surface of ZnO-QDs showed a simple, reproducible and reliable process, which represents an important aspect in the surface modification of QDs. This is possible due to one only step that can be achieved in function of hydrolysis and condensation reaction in room temperature and under basic catalysis between the ZnO-QDs and siloxane groups present in the organosilanes, thus providing a capped ZnO-QDs precipitate in the ethanolic medium of colloidal ZnO-QDs, which also can be related with epoxy end group of GPTMS. Figure 1 illustrates the capping methods used for passivation of ZnO-QDs by organosilanes and AO.

The bonding structure of modified ZnO-QDs powder was analyzed by FTIR spectroscopy. According to Spanhel and Anderson [25], the ZnO-QDs sol–gel synthesis is quite complex involving the formation of acetate groups and other by-products that can be adsorbed on ZnO-QDs surface. For all capped samples, the figure 2 shows a broad IR absorption band, characteristic of hydroxyl (OH) groups, at about 3400 cm^{-1}, peaks related to stretching modes (symmetric and asymmetric) of acetate group (COO^-), in the range of 1400–1600 cm^{-1}, and of C–H stretching modes (symmetric and asymmetric) in the 2942–2857 cm^{-1} range [28–30]. The peak at 870 cm^{-1} is related to symmetrical stretching mode of Zn–O–Si bonds, suggesting the successful covalent modification of ZnO-QDs surface by organosilanes [16, 23]. With increasing amount of GMPTS (figures 2(a)–(c)) this band increases, indicating the formation of a thicker capping layer.

The optical properties of capped ZnO-QDs have been investigated using UV–vis absorption spectroscopy, which allows to identify the wavelength limit associated with the excitonic peak [31]. The method, suggested by Nedelijkovic *et al* [32], utilizes the intersection of peak tangent with wavelength axis to determine the cut-off wavelength. ZnO-QDs colloidal suspension show a well-defined excitonic peak within the limit wavelength near 355 nm typical for ZnO NPs [33] (supplementary data figure S1). The well-defined excitonic peak of capped ZnO-QDs by GPTMS in water and of ZnO-QDs modified by HTMS and OA/HTMS bilayer in chloroform appears at slightly higher wavelength, near 360 nm (supplementary data figures S2(a)–(d)).

The wavelength limit (λc) is related with the energy of band gap ($E_g = hc/\lambda c$) and using the model proposed by Brus [34], it was possible to calculate the average size of NPs. The model is based on the confinement of first excited electronic state, which can be approximated by equation (1).

$$E_g = E_g^{bulk} + \frac{h^2\pi^2}{2er^2}\left(\frac{1}{m_e^* m_0} + \frac{1}{m_h^* m_0}\right) - \frac{1.86}{4\pi\varepsilon\varepsilon_0 r} - \frac{0.124e^3}{h^2(4\pi\varepsilon\varepsilon_0)^2}\left(\frac{1}{m_e^* m_0} + \frac{1}{m_h^* m_0}\right) - 1 \quad (1)$$

Where, $E_g = 3.4$ eV is the particle energy gap (bulk); h is the Plank constant; r the particle radius; e the electron charge; ε_0 the vacuum permittivity; $\varepsilon = 3.7$ the relative permittivity; m_e free electron mass; $m_e^* = 0.24$ the effective electron mass; and $m_h^* = 0.45$ the effective hole mass.

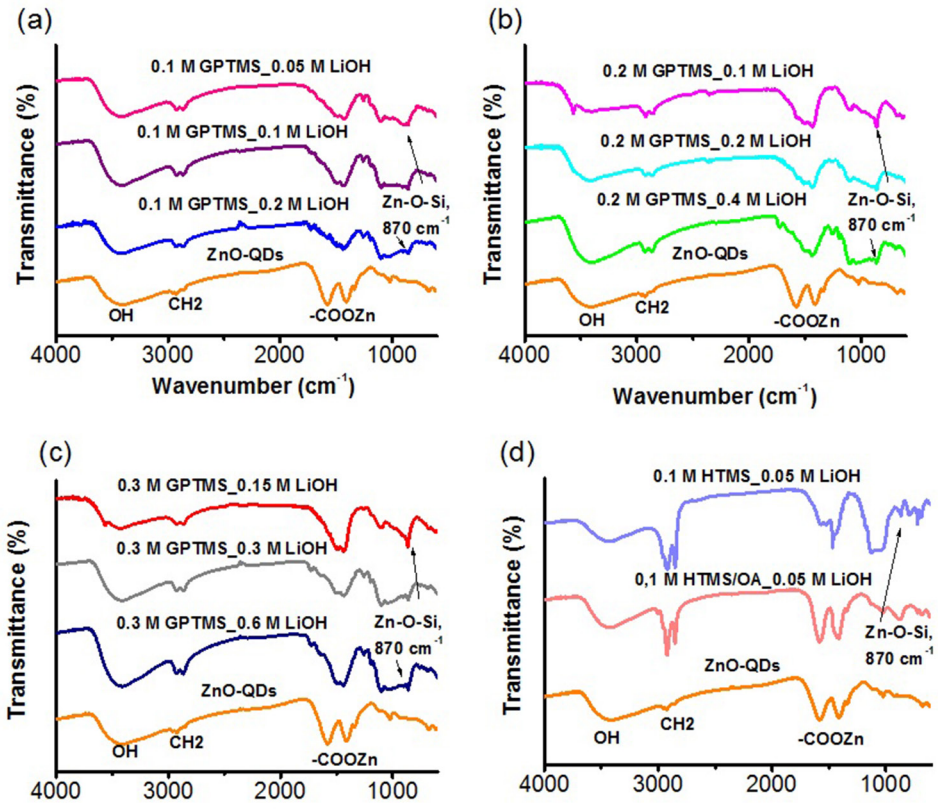

Figure 2. FT IR spectra of capped ZnO-QDs by GPTMS ((a)–(c)) and capped ZnO-QDs by HTMS and OA/HTMS bilayer (d).

The average particle size ($2r$) calculated form equation (1) was ~2.3 nm for ZnO-QDs in colloidal suspension and about 3 nm for the capped ZnO-QDs.

In addition, using UV–vis spectroscopy, the stability of the NPs was studies analyzing possible time dependent changes of the excitonic peak position for ZnO-QDs capped by GPTMS in water (supplementary data figures S3(a)–(d); figures S4(a)–(d); figure S5(a)) and OA/HTMS and HTMS in chloroform (supplementary data figures S5(b) and (c)). The results show that the absorbance profile and the size of most capped ZnO-QDs remained essentially unchanged during the study period of 15 d. These results can be explained by the protective effect of the siloxane layer formed around ZnO, which effectively prevents the aggregation of NPs [16]. Similar stability was also observed for ZnO-QDs modified by (poly) aminoalkoxysilane that exhibited intense photoluminescence and good stability in aqueous solution during 14 d [16, 23]. For 0.3 M GPTMS_0.6 M LiOH sample, however, a strong decline of the excitonic peak was observed after 7 d (figure S4(c)). This instability in water may be associated to the excess of LiOH in relation to GPTMS. A similar effect was reported by Innocenzi *et al* [35], who demonstrated that in highly basic condition, GPTMS suffer a quick hydrolysis and condensation, contributing to the formation of a porous silica matrix that reduces the protection around NPs thus favoring the agglomeration of ZnO nanoparticles.

Figures 3(a)–(c) shows the micrographs of three samples containing different concentrations of the GPTMs modifier, while figures 4(a) and (b) displays ZnO-QDs capped by a HTMS and OA/HTMS bilayer. The results show a spherical appearance of the NPs independently of modifier used. The average size, determined from the analysis of the micrographs, was in the range of 3.5–4 nm for the GPTMS capped ZnO-QDs (figures 3(a1)–(c1)) and 4.5 nm for ZnO-QDs the capped by HTMS and OA/HTMS bilayer (figures 4(a1) and (b1)). These results obtained for NPs modified with a shielding barrier by organosilanes are slightly higher than the values found using the model proposed by Brus [34], which provides the NPs size as a function of excitonic peak position, related purely to ZnO.

Figure 5 shows the XRD patterns for the capped ZnO-QDs by GPTMS (figure 5(a)) and those capped by a HTMS and OA/HTMS bilayer (figure 5(b)). The peak positions of different crystalline planes indicate the presence of a wurtzite crystal structure [16, 23, 25]. In general, due to the small size of the crystallites, the peaks in are quite broad and are poorly defined. With increasing GPTMS concentration was increased, new peaks appeared in 33, 52 and 56°, indicating the formation of a new crystalline phase (figure 5(a)). Furthermore, the presence of well-defined peak at 22° for the capped ZnO-QDs by HTMS and OA/HTMS bilayer indicates the formation of a HTMS layer surrounding the ZnO core, as observed in the study realized by Li *et al* [16].

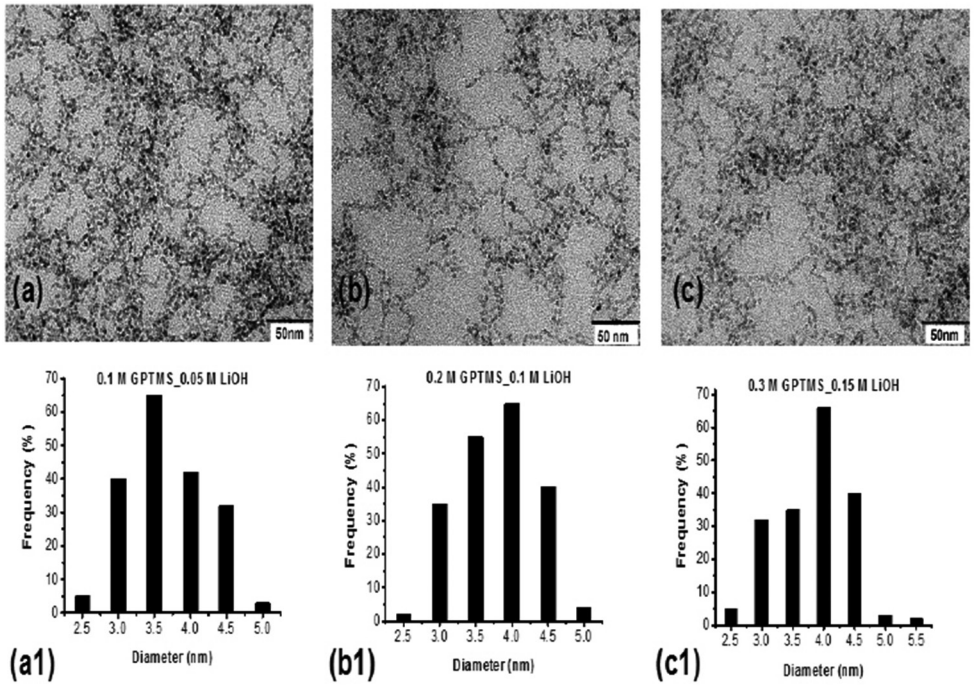

Figure 3. Transmission electron microscopy (TEM) of capped ZnO-QDs by GPTMS ((a)–(c)) and an average size of NPs ((a1)–(c1)).

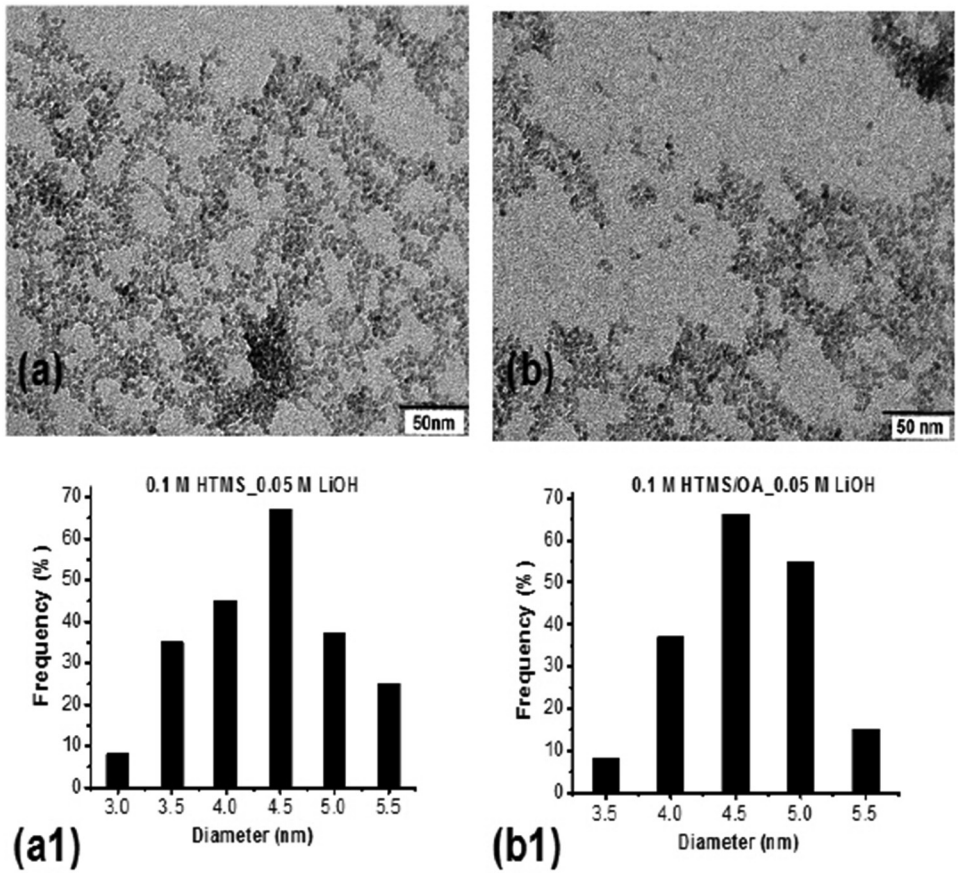

Figure 4. TEM of capped ZnO-QDs by HTMS and OA/HTMS bilayer ((a) and (b)) and an average size of NPs ((a1) and (b1)).

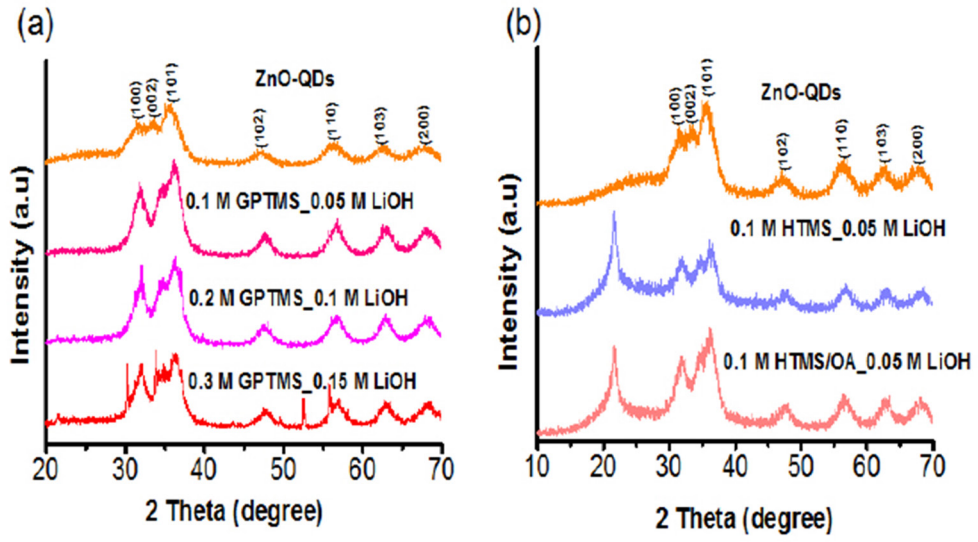

Figure 5. XRD data for the capped ZnO-QDs by GPTMS (a) and capped ZnO-QDs by HTMS and OA/HTMS bilayer (b).

Table 1. Atomic concentrations in percentage of the photoelectrons: Zn 2p, O1s, C1s e Si 2p.

	ZnO-QDs	0.1 M GPTMS_ 0.05 M LiOH	0.2 M GPTMS_ 0.1 M LiOH	0.3 M GPTMS_ 0.15 M LiOH (at.%)[a]	0.1 M HTMS_ 0.05 M LiOH	0.1 M HTMS/ OA_ 0.05 M LiOH
Zinc	27.4	25.3	20.5	20.6	4.0	19.1
Oxygen	46.5	40.1	41.5	43.6	13.4	22.5
Carbon	26.1	29.5	33.5	30.6	76.8	56.6
Silicium	—	4.1	4.5	5.2	5.8	1.7
Zn/Si	—	6.2	4.6	3.9	0.7	11.2

[a]Exp. error ±5%.

The chemical bonding structure, as well as the atomic concentration of elements of bare ZnO-QDs and capped ZnO-QDs was investigated by XPS. As the XPS sampling depth is about 5 nm, which is comparable to the NPs size (3–4 nm), the technique allowed to investigate the entire NP volume.

Atomic concentrations of elements of the capped and bare ZnO-QDs are displayed in table 1. It can be observed that samples containing GPTMS showed a decrease in zinc and oxygen concentration, as the concentration of GPTMS was increased, indicating the formation of a thicker siloxane layer atop ZnO-QDs, also expressed by the decreasing Zn/Si ration (table 1). The much smaller concentration of Zn and O detected for the HTMS capped sample indicates a significantly larger attenuation effect of the Zn 2p and O1s photoelectron intensity. Together with the strong increase of the carbon content, this composition profile evidences a complete grafting of the ZnO-QDs with a well-organized molecular structure of HTMS with the hydrocarbon tail pointing in the radial direction. The lowest Si content of only 1.7 at.%, detected for the capped ZnO-QDs by OA/HTMS, confirms the formation of a bilayer. However, the higher Zn concentration indicates the bilayer might not be distributed homogenous around the NPs.

Further information on the ZnO-QDs was obtained analyzing the local bonding structure. The main intensity of the deconvoluted Zn 2p spectrum of ZnO-QDs at 1021.7 eV is related to the ZnO phase and the small component at 1023.4 eV, it was attributed to surface zinc hydroxide (supplementary data figure S6(a)). In the O1s spectrum the presence of O–Zn bond was identified at a binding energy of 530.1 eV, characteristic for the ZnO phase. The main intensity at 531.7 eV is related to surface hydroxyl groups of ZnO-QDs and a small contribution of O = C bonds of oxygenated carbon groups of adventitious carbon, appearing at 532.7 eV and 533.8 eV, as O–C an O–C=O, respectively (supplementary data figures S6(b)). It is possible that a part of the carbonyl (C=O) and acetate (O–C=O) groups come from the acetate precursor of the ZnO colloidal suspension, formed during the sol–gel process.

The XPS spectra of samples capped by the siloxane layer show the signal of silicon (Si 2p), with as single component at 102.2 eV, associated with C–SiO_x bonds of GPTMS an HTMS (supplementary data figures S7(d), S8(d), S9(d), S10(d) and S11(d)). The C1s spectra of these samples capped by GPTMS confirm in addition to the contribution of hydrocarbon groups (285.0 eV) also the strong presence of epoxy C–O bonds at 286.5 eV (supplementary data figures S7(c), S8(c) and S9(c)). For ZnO-QDs capped by HTMS and the OA/HTMS bilayer, the C1s

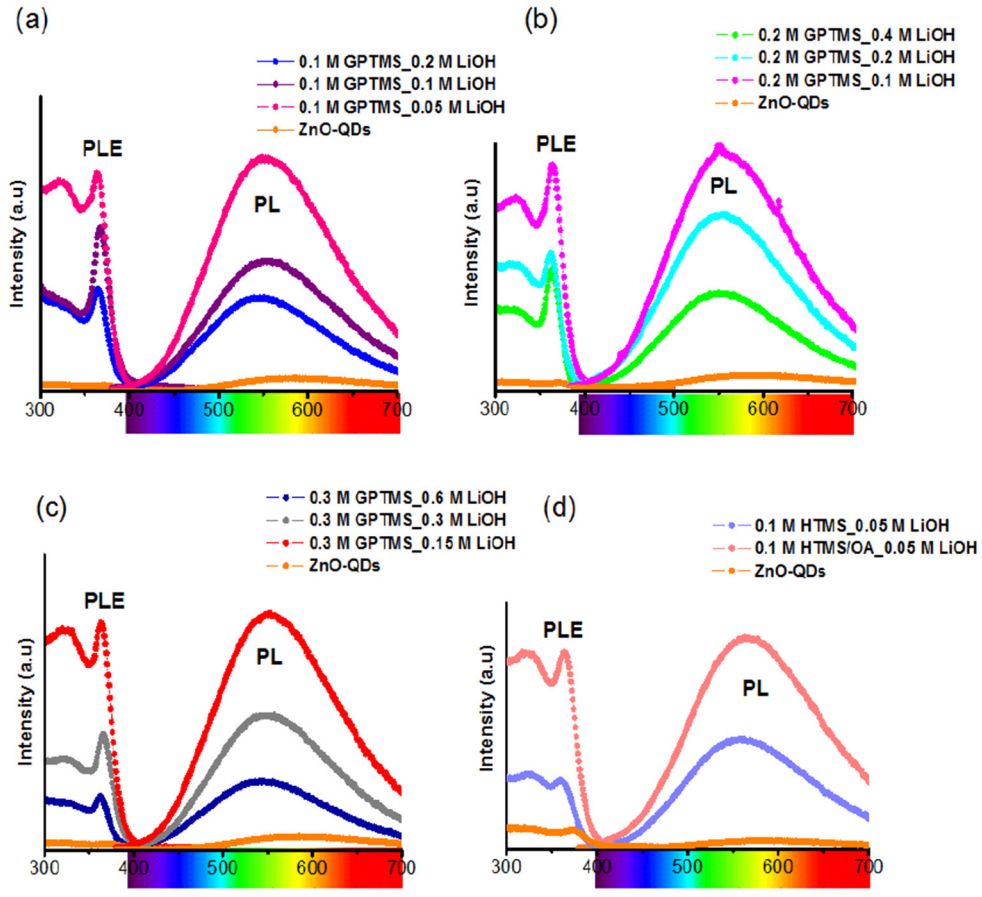

Figure 6. Excitation spectra (PLE) and emission spectra (PL) of capped ZnO-QDs by GPTMS ((a)–(c)) and capped ZnO-QDs by HTMS and OA/HTMS bilayer (d).

spectra evidence the predominant presence of hydrocarbon groups of the polymeric tail of HTMS (supplementary data figure S10(c) and S11(c)).

A clear evidence for the formation of Zn–O–Si bonds between ZnO-QDs and the siloxane capping layer was obtained from the analysis of the O1s spectra. Despite the fact that no significant shift of the Zn 2p peak the position (1021.7 eV) in relation to bare ZnO-QDs was observed, the O1s spectra show for all capped samples a strong decrease of the of the intensity of surface hydroxyl groups, located at 531.7 eV, accompanied by a strong increase of O–Zn bonds at 530.1 eV, thus indicating of covalent Zn–O–Si bond between the zinc oxide and the silica phase.

From photoluminescence experiments, it was possible to obtain relevant information regarding the electron energy levels within in the band gap, derived from the intensity and peak position of the photoluminescence bands. Figure 6 shows the excitation intensity of capped ZnO-QDs powder with the main peak at 365 nm, followed by emission spectra, which showed an emission centered in the green spectral range at 550 nm. In contrast, bare ZnO-QDs powder showed much lower photoluminescence intensity centered in the yellow spectral range at 580 nm. Also from spectra we found the values of integral area under a curve, as shown in table S1 (supplementary data).

The above values of integral area indicate that photoluminescence of capped ZnO-QDs by GPTMS was lower among the samples containing a higher concentration of LiOH. These results representing the importance of basic catalyst to the organization of siloxane layer around the NPs and consequently in the reduction of surface defects. The lower values found for the samples containing a higher concentration of GPTMS might be related with excess of their molecules around the NPs. In addition, it was observed that the bilayer organization among OA/HTMS can be related with the increasing in photoluminescence and was reported by Li *et al* [16].

The lower photoluminescence intensity in the yellow spectral range for bare ZnO-QDs probably occurred during acquisition of the ZnO-QDs in powder form. The above results are different from that found for the ZnO-QDs colloidal suspension prepared by sol–gel route, which having shown a great photoluminescence in the green spectral range [36]. This phenomenon might be related with the security of NPs in function of colloidal protection, which is lost after the ZnO-QDs powder obtaining. The stability of the photoluminescence properties of capped ZnO-QDs can be primarily related to the improved stability that the capping provides to the NPs, even after they were submitted to drying process Additionally, the increase of the photoluminescence intensity and the green-shift observed for ZnO-QDs capped with increasing quantities of GPTMS can be related to a shift of the oxygen

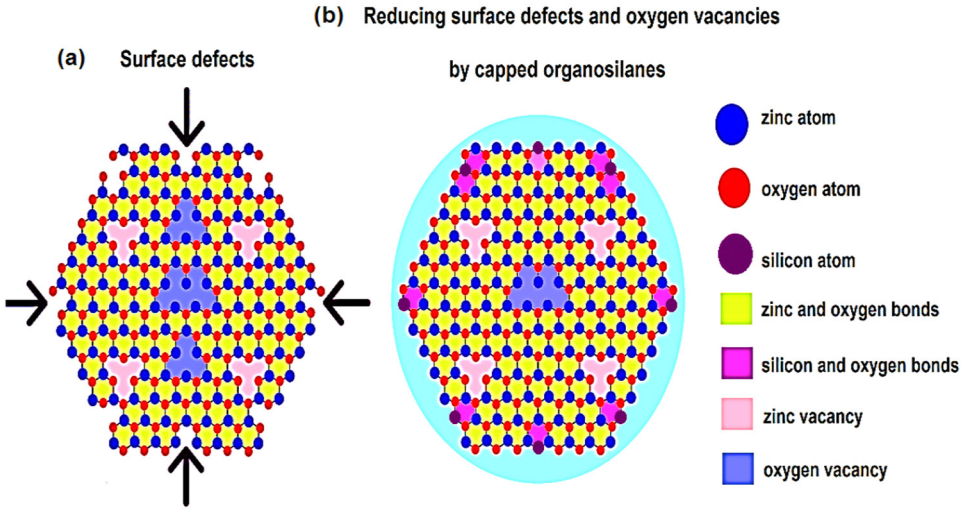

Figure 7. ZnO-QDs crystal structure containing surface defects and intrinsic defects (a) and reducing of these defects by surface passivation with organosilanes (b).

vacancy levels accompanied by a decrease trap levels density induced by surface defect, healed by the capping layer. This implies that the use of organosilanes as passivation agents significantly contributes to photoluminescence enhancement and stability of ZnO-QDs, especially in aqueous media [16, 20–24, 27].

The increase of the photoluminescence intensity found for the capped ZnO-QDs corroborates with results reported by Moghaddam *et al* [27]. Using aminopropyltriethoxysilane (APTES) for passivation of ZnO-QDs surface, the authors suggested that the photoluminescence stability might result from the reduction of the intrinsic defects in ZnO-QDs. It is likely that the alkaline medium used in the hydrolysis and condensation reaction of APTES and the resulting interaction with the ZnO-QDs surface could have generated oxygen anions, completing the oxygen vacancies (V_o). Consequently, the improved stability and reduction of intrinsic and extrinsic surface defects, as represented by figure 7, are the principal factors that contribute to the high photoluminescence yield.

The ratio of emitted photons by absorbed photons number was analyzed using quantum yield (QY) of capped ZnO-QDs by GPTMS in water and capped ZnO-QDs by HTMS and OA/HTMS bilayer in chloroform comparing to ZnO-QDs colloidal suspension. According to method described by Demas and Crosby [37] and by following equation (2), it was possible calculated the QY of this samples.

$$\mathrm{QY}_x = Q_\mathrm{r}\,[A_x/A_\mathrm{r}]\left(\frac{n_x^2}{n_\mathrm{r}^2}\right) \tag{2}$$

Where, $\mathbf{QY_r} = 0.95$ (quantum yield rhodamina 6G); $\boldsymbol{A_x}$ = photoluminescence area of sample; $\boldsymbol{A_r}$ = photoluminescence area of rhodamina 6G; $\boldsymbol{n_x^2}$ = solvent refractive index at which the sample is dispersed; $\boldsymbol{n_r^2}$ = solvent refractive index at which rhodamina 6G is dispersed.

QY results showed that the surface modifiers do not interfere significantly when compared to the ZnO-QDs colloidal suspension (10.2%), which corroborated with the QY reported by Manaia *et al* [36]. The results related with ZnO-QDs capped by GPTMS and HTMS can be explained by reduction of defects present in the crystal structure (as seen above). This effect was observed, especially for the sample of 0.2 M LiOH GPTMS_0.1 M, which showed a higher yield (10.8%). The QY of 6.8% found for the 0.3 M LiOH GPTMS_0.15 M might be related with an excess of GPTMS that may have saturated the surface of NPs, thus decreasing the photoluminescence, the other QY results are displayed in table S2 (see supplementary data). The best result found for the capped ZnO-QDs by OA/HTMS can be explained by bilayer formation around the NPs. This result was also supported by Li *et al* [16], due to bilayer formed between the HTMS and aminopropyltriethoxysilane (APS). According to the study the use of a hydrophobic modifier around the core and functionalized with a hydrophilic modifier provided to NPs a great stability and also an enhanced fluorescence intensity in approximately 10 times compared to unprotect ZnO in water, thus promising their application in the optical and biological fields.

4. Conclusions

The sol–gel process was used to successfully synthetize of crystalline capped ZnO-QDs by a siloxane capping layers formed by hydrolysis and condensation of GPTMS and a combination of HTMS and oleic acid precursors. TEM and UV–Vis spectroscopy confirmed the presence of well-dispersed nanoparticles with a size of 3–4.5 nm. The analysis of the composition and the local bonding structure, performed by FTIR and XPS, evidenced the formation

of homogeneous capping layers interacting by covalent Zn–O–Si bonds with the Zinc oxide surface. The obtained results for different passivation methods of have shown that the applied method is very promising in terms of a significant improvement the stability of ZnO-QDs and reduction of their surface defect density of surface states, resulting to a substantial enhancement of the photoluminescence yield. Overall, the results presented in this work indicate the great potential of capped ZnO-QDs for the application as biological probe, since principally the stability of ZnO-QDs in water grantees their use in various biological applications. Finally, the possibility of encapsulation of siloxane capped ZnO-QDs in amphiphilic systems can contribute to development of theranostics systems.

Acknowledgments

FAPESP, CAPES, PADC/FCF, TEM facilities provided by LME-IQ-UNESP.

References

[1] Frasco M F and Chaniotakis N 2010 Bioconjugated quantum dots as fluorescent probes for bioanalytical applications *Anal. Bioanal. Chem.* **396** 229–40
[2] Zhang J, Zhao S-Q, Zhang K and Zhou J-Q 2014 Cd-doped ZnO quantum dots-based immunoassay for the quantitative determination of bisphenol A *Chemosphere* **95** 105–10
[3] Zhao D, Song H, Hao L, Liu X, Zhang L and Lv Y 2013 Luminescent ZnO quantum dots for sensitive and selective detection of dopamine *Talanta* **107** 133–9
[4] Wang L, Sun Y, Wang J, Wang J, Yu A, Zhang H and Song D 2010 Water-soluble ZnO–Au nanocomposite-based probe for enhanced protein detection in a SPR biosensor system *J. Colloid Interface Sci.* **351** 392–7
[5] Ghasemi Y, Peymani P and Afifi S 2009 Quantum dot: magic nanoparticle for imaging, detection and targeting *Acta Bio Med. Atenei Parmensis* **80** 156–65
[6] Woggon U 1997 *Optical Properties of Semiconductor Quantum Dots* (Berlin: Springer)
[7] Samir T M, Mansour M M H, Kazmierczak S C and Azzazy H M E 2012 Quantum dots: heralding a brighter future for clinical diagnostics *Nanomedicine* **7** 1755–69
[8] Sahai A and Goswami N 2014 Probing the dominance of interstitial oxygen defects in ZnO nanoparticles through structural and optical characterizations *Ceramics International* **40** 14569–78
[9] Janotti A and Van de Walle C G 2009 Fundamentals of zinc oxide as a semiconductor *Rep. Prog. Phys.* **72** 126501
[10] Wang Y, Zhang Y and Zhang W 2014 First-principles study of the halide-passivation effects on the electronic structures of CdSe quantum dots *RSC Adv.* **4** 19302–9
[11] Bera D, Qian L, Tseng T-K and Holloway P H 2010 Quantum dots and their multimodal applications: a review *Materials* **3** 2260–345
[12] Talapin D V, Rogach A L, Kornowski A, Haase M and Weller H 2001 Highly luminescent monodisperse CdSe and CdSe/ZnS nanocrystals synthesized in a hexadecylamine-trioctylphosphine oxide-trioctylphospine mixture *Nano Lett.* **1** 207–11
[13] Qu L, Peng Z A and Peng X 2001 Alternative routes toward high quality CdSe nanocrystals *Nano Lett.* **1** 333–7
[14] Kumari K, Kumar U, Sharma S N, Chand S, Kakkar R, Vankar V D and Kumar V 2008 Effect of surface passivating ligand on structural and optoelectronic properties of polymer: CdSe quantum dot composites *J. Phys. D: Appl. Phys.* **41** 235409
[15] Wang C, Gao X and Su X 2010 *In vitro* and *in vivo* imaging with quantum dots *Anal. Bioanal. Chem.* **397** 1397–415
[16] Li S, Sun Z, Li R, Dong M, Zhang L, Qi W, Zhang X and Wang H 2015 ZnO nanocomposites modified by hydrophobic and hydrophilic silanes with dramatically enhanced tunable fluorescence and aqueous ultrastability toward biological imaging applications *Sci. Rep.* **5** 8475
[17] Gulia S and Kakkar R 2013 ZnO quantum dots for biomedical applications *Adv. Mater. Lett.* **4** 876–87
[18] Moussodia R-O, Balan L and Schneider R 2008 Synthesis and characterization of water-soluble ZnO quantum dots prepared through PEG-siloxane coating *New J. Chem.* **32** 1388–93
[19] Moussodia R-O, Balan L, Merlin C, Mustin C and Schneider R 2010 Biocompatible and stable ZnO quantum dots generated by functionalization with siloxane-core PAMAM dendrons *J. Mater. Chem.* **20** 1147–55
[20] Jana N R, Earhart C and Ying J Y 2007 Synthesis of water-soluble and functionalized nanoparticles by silica coating *Chem. Mater.* **19** 5074–82
[21] Jana N R, Yu H-h, Ali E M, Zheng Y and Ying J Y 2007 Controlled photostability of luminescent nanocrystalline ZnO solution for selective detection of aldehydes *Chem. Commun.* **2007** 1406–8
[22] Wu Y L, Tok A I Y, Boey F Y C, Zeng X T and Zhang X H 2007 Surface modification of ZnO nanocrystals *Appl. Surf. Sci.* **253** 5473–9
[23] Aboulaich A, Tilmaciu C-M, Merlin C, Mercier C, Guilloteau H, Medjahdi G and Schneider R 2012 Physicochemical properties and cellular toxicity of (poly) aminoalkoxysilanes-functionalized ZnO quantum dots *Nanotechnology* **23** 335101
[24] Bruce I J and Sen T 2005 Surface modification of magnetic nanoparticles with alkoxysilanes and their application in magnetic bioseparations *Langmuir* **21** 7029–35
[25] Spanhel L and Anderson M A 1991 Semiconductor clusters in the sol–gel process: quantized aggregation, gelation, and crystal growth in concentrated zinc oxide colloids *J. Am. Chem. Soc.* **113** 2826–33
[26] Meulenkamp E A 1998 Synthesis and growth of ZnO nanoparticles *J. Phys. Chem.* B **102** 5566–72
[27] Moghaddam E, Youzbashi A A, Kazemzadeh A and Eshraghi M J 2015 Preparation of surface-modified ZnO quantum dots through an ultrasound assisted sol–gel process *Appl. Surf. Sci.* **346** 111–4
[28] Jimenez-Gonzalez A E, Urueta J A S and Suarez-Parra R 1998 Optical and electrical characteristics of aluminum-doped ZnO thin films prepared by solgel technique *J. Cryst. Growth* **192** 430–8
[29] Sharma A, Singh B P, Dhar S, Gondorf A and Spasova M 2012 Effect of surface groups on the luminescence property of ZnO nanoparticles synthesized by sol–gel route *Surf. Sci.* **606** L13–7
[30] Xiong G, Pal U and Serrano J G 2007 Correlations among size, defects, and photoluminescence in ZnO nanoparticles *J. Appl. Phys.* **101** 024317
[31] Yu W W, Qu L, Guo W and Peng X 2003 Experimental determination of the extinction coefficient of CdTe, CdSe, and CdS nanocrystals *Chem. Mater.* **15** 2854–60

[32] Nedelijkovic J M, Patel R C, Kaufman P, Joyce-Pruden C and O'Leary N 1993 Synthesis and optical properties of quantum-sized metal sulfide particles in aqueous solution *J. Chem. Educ.* **70** 342
[33] Pesika N S, Hu Z, Stebe K J and Searson P C 2002 Quenching of growth of ZnO nanoparticles by adsorption of octanethiol *J. Phys. Chem.* B **106** 6985–90
[34] Brus L E 1983 A simple model for the ionization potential, electron affinity, and aqueous redox potentials of small semiconductor crystallites *J. Chem. Phys.* **79** 5566–71
[35] Innocenzi P, Figus C, Kidchob T, Valentini M, Alonso B and Takahashi M 2009 Sol–gel reactions of 3-glycidoxypropyltrimethoxysilane in a highly basic aqueous solution *Dalton Trans.* **42** 9146–52
[36] Manaia E B, Kaminski K, Cristina R, Caetano B L, Briois V, Chiavacci L A and Bourgaux C 2015 Surface modified Mg-doped ZnO QDs for biological imaging *Eur. J. Nanomed.* **7** 109–20
[37] Demas J N and Crosby G A 1971 Measurement of photoluminescence quantum yields-review *J. Phys. Chem.* **75** 991